Photochemical & Photobiological Sciences

Accepted Manuscript

This is an *Accepted Manuscript*, which has been through the Royal Society of Chemistry peer review process and has been accepted for publication.

Accepted Manuscripts are published online shortly after acceptance, before technical editing, formatting and proof reading. Using this free service, authors can make their results available to the community, in citable form, before we publish the edited article. We will replace this *Accepted Manuscript* with the edited and formatted *Advance Article* as soon as it is available.

You can find more information about *Accepted Manuscripts* in the Information for Authors.

Please note that technical editing may introduce minor changes to the text and/or graphics, which may alter content. The journal's standard Terms & Conditions and the Ethical guidelines still apply. In no event shall the Royal Society of Chemistry be held responsible for any errors or omissions in this *Accepted Manuscript* or any consequences arising from the use of any information it contains.

ROYAL SOCIETY OF CHEMISTRY

www.rsc.org/pps

Steady state and time-resolved photophysical study of CdTe quantum dots in water.

Alessandro Iagatti,[a;b] Luigi Tarpani,[c] Eleonora Fiacchi,[c] Laura Bussotti,[a] Agnese Marcelli,[a] Paolo Foggi[a;b;c] and Loredana Latterini[c*]*

[a]European Laboratory for Non Linear Spectroscopy (LENS), Università di Firenze, via Nello Carrara 1, 50019 Sesto Fiorentino, Florence, Italy

[b]INO-CNR, Istituto Nazionale di Ottica – Consiglio Nazionale delle Ricerche, Largo Fermi 6, 50125 Florence, Italy

[c]Dipartimento di Chimica, Biologia e Biotecnologie and Centro Eccellenza Materiali Innovativi Nanostrutturati (CEMIN), Università di Perugia, Via Elce di Sotto 8, 06123 Perugia, Italy

E-mail: loredana.latterini@unipg.it ; foggi@lens.unifi.it

The non-radiative electron-hole recombination processes are predominant in alkyl-thiol capped CdTe QDs prepared in water due and they are affected by the nature of the capping agent.

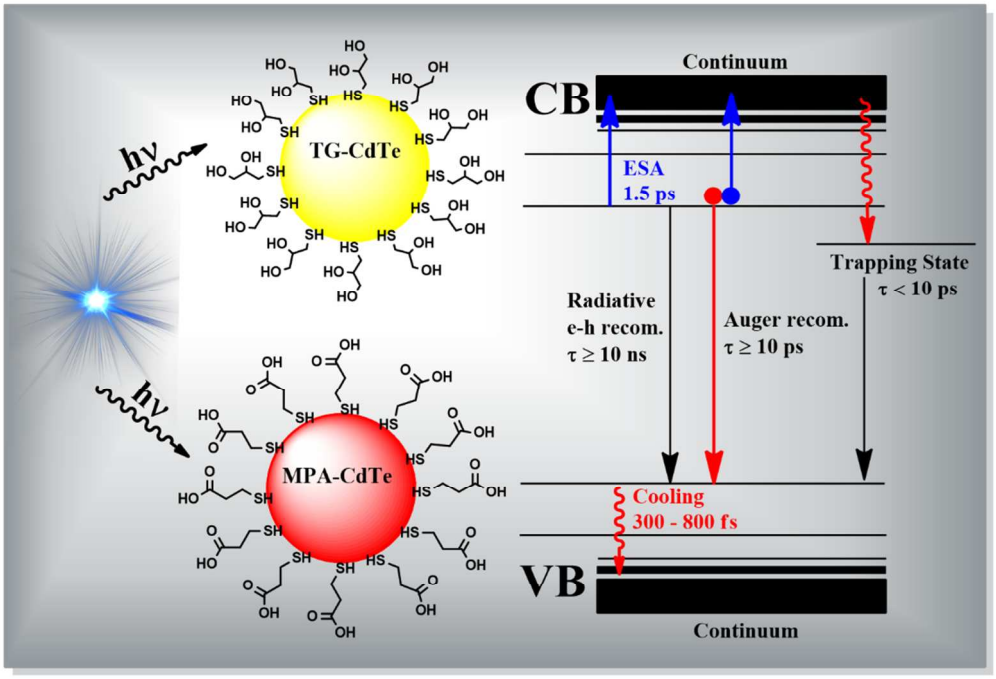

Steady state and time-resolved photophysical study of CdTe quantum dots in water.

Alessandro Iagatti,[a;b] *Luigi Tarpani,*[c] *Eleonora Fiacchi,*[c] *Laura Bussotti,*[a] *Agnese Marcelli,*[a] *Paolo Foggi*[a;b;c*] *and Loredana Latterini*[c*]

[a]European Laboratory for Non Linear Spectroscopy (LENS), Università di Firenze, via Nello Carrara 1, 50019 Sesto Fiorentino, Florence, Italy

[b]INO-CNR, Istituto Nazionale di Ottica – Consiglio Nazionale delle Ricerche, Largo Fermi 6, 50125 Florence, Italy

[c]Dipartimento di Chimica, Biologia e Biotecnologie and Centro Eccellenza Materiali Innovativi Nanostrutturati (CEMIN), Università di Perugia, Via Elce di Sotto 8, 06123 Perugia, Italy

E-mail: loredana.latterini@unipg.it ; foggi@lens.unifi.it

Keywords: CdTe Nanocrystals, Mercapto-derivatives, Capping Agent, Luminescence, Ultrafast Transient Absorption Spectroscopy.

Abstract

The exciton generation and recombination dynamics in semiconductor nanocrystals is very sensitive to small variations of dimensions, shape and surface capping. In the present work CdTe quantum dots are synthesized in water using 3-mercaptopropionic acid and 1-thioglycerol as stabilizers. Nanocrystals with an average dimension of 4±1 and 3.7±0.9 nm are obtained, when 3-mercaptopropionic acid or 1-thioglycerol, respectively was used as capping agent. The steady-state characterizations show that the two types of colloids have different luminescence behavior. In order to investigate the electronic structure and the dynamics of the exciton state, a combined study in the time domain has been carried out by use of fluorescence time-correlated single photon counting and femtosecond transient absorption techniques.

The electron-hole radiative recombination occurs following a non-exponential decay law for both colloids, which results in different average decay time values (on the order of tens of nanoseconds) for the two samples. The data demonstrate that the process is slower for 1-thioglycerol-stabilized colloids.

The ultrafast transient absorption measurements are performed at two different excitation wavelengths (at the band gap and at higher energies). The spectra are dominated in both types of samples by the negative band-gap bleaching signals although transient positive absorption bands due to the electrons in the conduction band are observable. The analysis of the signals is affected by the different interactions with the defect states, due to ligand capping capacities. In particular, the data indicate that in 1-thioglycerol-stabilized colloids the non-radiative recombination processes are kinetically more competitive than the radiative recombination. Therefore the comparison of the data obtained for the two samples are interpreted in terms of the effects of the capping agents on the electronic relaxation of the colloids.

Introduction

The design of hybrid nanomaterials based on colloidal semiconductor nanocrystals (or quantum dots, QDs) and organic moieties has attracted prominent attention in the last three decades due to their unique physical and chemical properties. Several different synthetic methods have been developed to obtain such materials. In wet synthetic procedures, the control of the nucleation and growth processes is achieved by using organic capping agents. These species have therefore a crucial role in determining the dimension and the structure properties of the colloidal nanocrystals. The detailed investigations of the effects of the capping agents enabled the development of a wide variety of researches and different applications [1–7]. At the same time a deeper understanding of the influence of stabilizers on the chemical and physical properties of colloids has been achieved [8-13]. It is now clear that ligand molecules affect the lattice properties of the colloids as well as the nanocrystal growth process [14]. So far the influence of the ligand molecules on the photophysical behaviour of QDs and on the dynamics of exciton state has been investigated to a lesser extent. Ligand exchange experiments have demonstrated that the luminescent and photophysical behavior of nanocrystals can be modified by the nature of the organic capping agents [15,16]. In order to produce hybrid nanomaterials based on QDs and organic ligands with defined behavior and functions, the interactions between semiconductor nanocrystals and organic species must be deeply understood.

Ultrafast pump-probe transient absorption spectroscopy (TAS) is a powerful tool for studying the relaxation processes of molecules and colloidal nanostructures at early stages after electronic excitation. Yan et al. [17] investigated the transient spectra of CdTe nanocrystals prepared by high temperature thermolysis; multiple bleaching signals dominate TA spectra and the electron cooling rates are reduced when the nanocrystals are capped with a CdS shell. This is due to a

reduction of the Auger recombination rates in the core/shell nanostructures, where the electron and hole are spatially separated.

In this context the use of TAS to explore the dynamics of CdTe colloids (obtained by mild thermolysis process assisted by organic thiol ligands) appears particularly interesting. Recent studies on CdTe QDs have been reported [18,19] in which the radiative and non-radiative recombination processes were investigated in the presence of 3-mercaptopropionic-acid as stabilizer.

In the present work we investigate the photophysics of CdTe QDs synthesized in water using 1-thioglycerol (1TG) and 3-mercaptopropionic-acid (MPA) as capping agents. The photophysical properties are investigated with stationary and time-resolved techniques. Stationary photoluminescence studies showed some differences among the samples, in terms of spectral features and efficiency values, which can be compatible with the presence of defect states. The combination of time correlated single photon counting (TCSPC) and UV/Vis TAS allows to characterize the radiative and non-radiative relaxation processes of charge carriers formed upon photoexcitation on a very wide time interval (from 100 fs to 100 ns).

Experimental Section

Materials

$Cd(NO_3)_2$ *$4H_2O$, 1-thioglycerol (1TG) and 3-mercaptopropionic-acid (MPA) are from Sigma-Aldrich. MilliQ water is freshly prepared in our laboratory.

Nanocrystal synthesis

CdTe QDs are prepared following literature procedures, with minor modifications [18, 20-22]. CdTe nanocrystals were prepared in strongly alkaline aqueous solution (pH=12) to ensure complete deprotonation of the ligands in order to have an higher coordination capacity. Briefly, the solutions of the reactants are freshly prepared as follows: 0.2 mmol of $Cd(NO_3)_2*4H_2O$ and 0.4 mmol of 1TG (or MPA) are added to a 40 ml of milliQ water under vigorous magnetic stirring. When the solution is well mixed, 1 M NaOH is added drop-wise till to obtain a pH value around 12; the solution of Te^{2-} precursor is prepared adding 0.4 mmol of tellurium powder and 1 mmol of $NaBH_4$ in 10 ml of milliQ water; the reduction is carried out at 80 °C under a nitrogen atmosphere.

The two stock solutions of the precursors are then mixed with a Cd/Te molar ratio of 1:1 in order to obtain the nanocrystals. The nucleation and the growth stage of the reaction is conducted at 100 °C in an inert atmosphere. The progress of the reaction is spectrophotometrically checked and the samples analyzed for particle dimensions.

Morphological Characterization

A Philips model 208 Transmission Electron Microscope (operating at 80 kV of beam acceleration) is used to image the nanocrystals and analyze their size distribution. A grain analysis is carried out to determine the height distribution of the particles from the images.

Photophysical Characterization

UV-VIS absorption spectra are recorded with a Perkin-Elmer Lambda 800 spectrophotometer on air-equilibrated solutions. Photoluminescence spectra, corrected for the instrumental response, are measured with a Fluorolog (Spex F112AI) spectrofluorometer, which are used to determine

photoluminescence efficiencies (QY) using quinine sulfate in H_2SO_4 (0.5 M), Φ_F = 0.55 as standard [15].

Time Correlated Single Photon Counting (TCSPC) measurements were performed to characterize the radiative electron-hole recombination. The luminescence decay (mean deviation of three independent experiments, ca. 5%) is measured by TCSPC method using an Edinburgh Instrument 199S setup. A 460-nm nanoLED with a 1.3 ns pulse duration was used as excitation source and the signal was acquired by a Hamamatsu R7400U-03 detector.

The apparatus used for TAS measurements has been described in detail in previous works [23-26]. Briefly, the fs-laser oscillator is a Ti:sapphire laser (Spectra Physics Tsunami). The short (≤70 fs) pulses are stretched and amplified at 1 kHz repetition rate by a regenerative amplifier (BMI Alpha 1000). After compression a total average power of 500 mW and pulse duration of 100 fs are obtained. The repetition rate of the output beam is reduced to 100 Hz by a mechanical chopper. Tunable pulses in the UV-Visible interval can be achieved by Second Harmonic Generation (SHG) or by doubling or mixing the output of an optical parametric generator and amplifier (OPG-OPA) based on a BBO crystal (TOPAS by Light Conversion, Vilnius, Lithuania)[27,28]. The probe pulse is generated by focusing a small portion of the 800 nm radiation on a 3 mm thick CaF_2 window mounted on a motorized translation stage. The continuum light is optimized for the 350-750 nm wavelength range. Multichannel detection for transient spectroscopy is achieved by sending the white light continuum, after passing through the sample, to a flat field monochromator coupled to a homemade CCD detector (see technical report at http://lens.unifi.it/ew/).

TAS measurements are carried out in a 2 mm thick cell under magnetic stirring to avoid the accumulation of long living transient species. To confirm the correct experimental conditions we optimize the stirring speed in order to reproduce results obtained in a flow cell [29-31].

The resulting kinetic traces are fitted by a multi-exponential decay function. For the short time scale the data are fitted by a decay function convoluted with a Gaussian-shaped instrument function (FWHM = 100 fs). To better evaluate the weight of the single components we first analyze the data by using a tail fitting procedure.

Results and Discussion

To investigate the photophysical behavior of CdTe nanocrystals (or quantum dots, QDs) in water, sample are prepared following the literature procedures [18, 20-22] using a [Cd]/[Te] molar ratio of 1, while the ratio between Cd and stabilizers has been fixed to 2. TEM images (inset Figure 1) show the formation of spherical nanocrystals, having an average size of 4±1 nm for 3-mercaptopropionic acid capped CdTe (MPA-CdTe) and 3.7±0.9 nm 1-thioglycerol was used as capping agent (TG-CdTe).

In Figure 1, the absorption and photoluminescence spectra of MPA and TG capped CdTe are shown. Both colloids present the band-gap absorption. However TG-CdTe samples show a better-defined band.

The lowest absorption bands of the samples are at 565 and 520 nm for MPA-CdTe and TG-CdTe, respectively. In addition both systems present the characteristic absorption due to the continuum. Following the model proposed by Donegá and Koole [32], the QDs extinction coefficient at 400 nm can be determined by the following equation:

$$\varepsilon_{400} = \left[\mu_{400} N_A z \frac{V_{QD}}{V_{UC}}\right] (2303)^{-1} \quad (1)$$

where μ_{400} is the absorption cross section per unit ion pair at 400 nm, N_A is the Avogadro's number, z is the number of unit ion pairs per unit cell, V_{QD} and V_{UC} are volumes (cm^3) of the QD and unit cell. Another method to determine the extinction coefficient ε of CdTe nanocrystals at the band gap has been developed by Peng et al. [33] and is given by the following empirical function:

$$\varepsilon = 3450\Delta E(D)^{2.4} \qquad (2)$$

where ΔE is the energy gap and D is the diameter of the nanoparticles. The absorption coefficient values calculated with the two methods are reported in Table 1 along with the QDs molar concentrations, determined using the Lambert-Beer law.

Since for both samples the concentration values are the same at the two wavelengths, within the experimental error, we conclude that the accuracy of the methods for the absorption coefficient determination is rather good. The comparison of the coefficients for the MPA- and TG-capped samples indicates that the nature of the capping agent has a moderate influence on the probabilities of the electronic transitions in the colloids, thus suggesting that the electronic structure of the nanocrystals is not altered by the presence of stabilizers of different nature.

The photoluminescence spectrum of the CdTe-MPA QDs obtained exciting the sample at the BG (565 nm) presents an emission band centered at 595 nm with a clear shoulder on the red edge (Figure 1A). The appearance of this component is generally ascribed to the contribution of trap states [15,16,34]. The occurrence of dissipative or trapping processes has been confirmed by the quite low luminescence efficiency measured (17%) for the CdTe-MPA suspension (Table 2). In addition we need to consider that a contribution to the red-edge component of the QDs luminescence due to the broad size distribution of these nanocrystals has to be taken into

account. The photoluminescence behavior of the TG capped QDs (Figure 1B), upon excitation of the nanocrystals at 520 nm, shows a single symmetric emission band centered at 560 nm. TG-CdTe QDs have an higher Stokes shift and a lower luminescence QY (10%) compared to MPA-capped samples. This is a proof that the luminescent properties of TG capped QDs are strongly affected by the presence of defects.

TCSPC measurements, carried out exciting the samples at 460 nm and collecting the photons at 620 nm, show a nonexponential behaviour of the luminescence decay curves, as previously observed for other colloidal samples [16,18,35-37]. The photoluminescence decays could be reproduced for both colloids by bi-exponential functions having decay time components in the ns range (7.1-51.0 ns, Table 3), which is a consequence of the distribution of radiative decay times related to excitonic populations [16,36,38].

The photoluminescence decay times, as well as the quantum yield, show some differences for the two samples under investigation. This suggests that the interactions with the organic ligands alters the dynamics of the exciton relaxation. In particular, longer decay times are measured for TG-CdTe, for which the presence of a larger amount of surface defects reducing the luminescence quantum efficiency (QY) has been expected on the basis of spectral features. Assuming that no other interactions occur within the excited states and considering the average decay times $<\tau_L>$ (Table 3) and the luminescence efficiencies, the average radiative (k_r) recombination rate constants can be determined for the two samples. For MPA- and TG-CdTe k_r values of 7.0 and 2.5×10^6 s^{-1}, respectively have been determined; on the other hand the average non-radiative rate constants (k_{nr}) operative for the excitonic state, determined considering $<\tau_L>$ and k_r, are in the order of 3.3 and 2.2×10^7 s^{-1} for MPA- and TG-capped colloids, respectively. The average data indicate that the non-radiative recombination pathway dominates the exciton

relaxation and a negligible effect has been observed on the non-radiative rates to account for the differences in the luminescence behavior. The lack of decay associated spectra prevents a more accurate analysis of the radiative and non-radiative rate constants; but it could be argued, on the basis of luminescence decay times values (Table 2), that for MPA-CdTe the radiative recombination is more competitive than for TG-CdTe since a faster luminescence component has been determined (7.1 ns).

To investigate in deeper details the dynamics of exciton states at short times, transient absorption measurements with fs-resolution have been carried out.

In TAS measurements, the excitation has been carried out at two wavelengths in order to have information on the relaxation processes in the manifold of the conduction band (CB). In particular, taking into account the steady-state absorption spectra of the CdTe colloids, the samples have been excited near the BG and at energies about 0.72 eV (5800 cm^{-1}) above the band gap (pump wavelength were set at 520 and 400 nm and 476 and 374 nm, for MPA- and TG-CdTe, respectively). It is important to notice that the pump power was kept below 100 nJ, with the aim to reduce multiexciton generation, whose dynamics would complicate the relaxation processes at least in the picosecond time window. The transient data of MPA-CdTe QDs recorded upon excitation at 520 and 400 nm are shown in Figure 2 and 3, respectively; the spectra of TG-CdTe are reported in Figures 4 and 5.

In general all the recorded transient spectra are dominated by the band gap bleaching signals but a broad excited state absorption (ESA) signal is also observed after the laser excitation pulse. In order to make easier the comparison in Figures 2-5A, the steady state absorption spectra of the samples are reported together with the transient spectra recorded 3 ps after the laser pulse.

Differently from what previously observed [17], the transient bleaching signals are broad and the contribution of selected electronic transitions could not be resolved.

The kinetic analysis has been carried out on the transient signals at different wavelengths. The ESA band is detected on the red-edge of the transient spectra (above 650 nm) and it forms instantaneously with excitation pulse. Data from the literature support the assignment of this ESA signal to the intraband transitions in CB [29]. The decay of the ESA signal can be satisfactorily reproduced by a double exponential function (Table 4) with a short component in the ps interval and a very long component (in the order of nanoseconds), which resemble the radiative decay times. This observation suggests that this signal can be assigned to the absorption of the electron in the conduction states which relax through the radiative process [19, 29].

More importantly, the bleaching signal generated upon CdTe excitation is due to charge carrier formation, thus its kinetic analysis gives more pieces of information on the dynamics of these species. It has to be noted that due to the difference between the masses of electron and holes, the dynamics is dominated by the electron relaxation. The bleaching analysis has been carried out at different wavelengths (Figure 2-5B) and the traces could be reproduced by multi-exponential functions, similarly to what previously observed for CdTe and CdSe QDs [11, 17, 19, 29, 39]. The traces evidenced a fast rise component, whose contribution (in amplitude and time) changed with the probe wavelength, and a quite complex decay, which was fitted by a triexponential function at all the probed wavelengths.

The rise component in the signal was reproduced by an exponential growth with a time constant τ_1 varying from 300 to 800 fs going from the blue to the red edge. This relaxation time is consistent with the electron cooling process into the VB. This assignment is supported by the red-shift of the maximum of the bleaching band in the first ps for both the particle types (Figure

6); a further proof of the assignment is the higher contribution (relative weight) of this component when the nanocrystals are excited at energies higher than the band gap.

Usually in QDs the fast non-radiative electron-hole recombination is dominated by surface trapping and/or Auger recombination [40-42]. Thus, in the present cases, the decay times τ_2 and τ_3 could be assigned to either to Auger recombination or to non-radiative recombination processes induced by the presence of defect states [10,18,40,43]. Increasing the pump power the decay time τ_2 remains constant, while the third component τ_3 shortens upon an increase of the laser power. These observations support the assignment of τ_2 to recombination assisted by the trap states and τ_3 to Auger recombination process [44]. These processes occur in both types of nanoparticles and a general scheme of the electronic transitions and relaxation processes can be drawn as reported in Figure 7.

The excitation of the samples with an excess of energy (400 nm for MPA and 374 nm for TG) compared to the BG transition originates similar transient spectral features, although some differences can be noticed in the fitting parameters obtained from the kinetic analysis. In particular, the decay time τ_2 shortens for both the colloids when the excitation wavelengths are set at higher energies. This decay behaviour, ascribed to the effect of trapping sites, is explained by the higher kinetic energy of the electrons into the conduction manifold when promoted with extra-energy. The τ_3 component becomes five times faster in MPA-CdTe increasing the excitation energy, but it does not change for the TG-CdTe; this behavior can be related to the higher absorption coefficients of MPA-CdTe at 400 nm which makes probable multi-exciton formation. However the contribution of a cooling process mediated by the ligand (non-adiabatic cooling) cannot be excluded at this stage. Indeed the τ_2 and τ_3 decay times are in general longer for MPA- than TG-CdTe. Thus, we can conclude that the presence of TG as capping agent, for

which a higher contribution of defect states is deduced from the luminescent behaviour, significantly reduces the two ps-components, suggesting that in this sample the non-radiative recombination processes are kinetically more competitive than the radiative recombination.

Conclusions

CdTe-QDs were prepared in water using two different alkyl-thiols as stabilizers, namely 3-mercaptopropionic acid (MPA) and 1-thioglycerol (TG). The optical properties of the two samples show significant differences, despite the similar dimensions. Indeed higher absorption coefficients and higher luminescent quantum efficiency have been determined for the MPA-CdTe while a larger stock-shift was measured for TG-QDs. These data suggest that luminescent behavior of TG-CdTe colloids is affects by the presence of defect states.

In order to explore if defects influence the electronic structure of the colloids or the dynamics of the exciton states, time resolved measurements have been carried out. The Time Correlated Single Photon Counting measurements indicate that the radiative electron-hole recombination occurs in the ns-time region with a bi-exponential behavior; the data analysis pointed out that exciton relaxation is kinetically determined by non-radiative cooling process.

The exciton dynamics was further studied with ultrafast Transient Absorption Spectroscopy monitoring the bleaching signal. The kinetic analysis of TAS signals at different probe wavelengths evidences a multiexponential recombination. At all analyzed wavelengths a rise time, in the order of hundreds of fs, was detected and assigned to the electron cooling in the VB. A decay component of few ps (τ_2) was ascribed to the trapping states, while the intermediate decay time (τ_3) was attributed to Auger recombination; the latter component presents the biggest

differences between the two samples. The identification of these processes is supported by pump fluence dependent measurements. In particular, the τ_3 component is almost one order of magnitude longer for MPA-CdTe.

Increasing the excitation energy a reduction of the τ_2 and τ_3 decay times was noticed for both the samples due to the increased mobility of the electrons in the conduction manifold. The increase is more evident for MPA-CdTe.

The comparison of the results obtained in QDs with two different stabilizers shows important differences in the non-radiative decay component and the contribution of a cooling process mediated by the ligand can be supposed.

Acknowledgments

The authors gratefully acknowledge the support of the University of Florence and the University of Perugia. A.I. and P.F. acknowledge the ENI S.P.A (Italy) and the Ministero per l'Università e la Ricerca Scientifica e Tecnologica (Rome, Italy) under the projects FIRB RBFR10Y5VW and EFOR L. 191/2009 art. 2 comma 44. L.L. thanks the financial support of Ministero per l'Università e la Ricerca Scientifica e Tecnologica (Rome, Italy) under the project PRIN 2010-2011, 2010FM738P.

References

1 A. J. Nozik, Nanoscience and nanostructures for photovoltaics and solar fuels, *Nano Lett.*, **2010**, 10, 2735–2741.

2 S. Rhle, M. Shalom and A. Zaban, Quantum-dot-sensitized solar cells, *ChemPhysChem*, **2010**, 11, 2290–2304.

3 K. Jeong, R. Pensack and J. Asbury, Vibrational spectroscopy of electronic processes in emerging photovoltaic materials, *Acc. Chem. Res.*, **2013**, 46, 1538–47.

4 K. Knowles, M. Peterson, M. McPhail and E. Weiss, Exciton dissociation within quantum dot-organic complexes: Mechanisms, use as a probe of interfacial structure, and applications *J. Phys. Chem. C*, **2013**, 117, 10229–10243.

5 K. Hyeon-Deuk and O. Prezhdo, Photoexcited electron and hole dynamics in semiconductor quantum dots: Phononinduced relaxation, dephasing, multiple exciton generation and recombination, *J. Phys. Condens. Matter*, **2012**, 24,363201.

6 K. Tvrdy and P. Kamat, Substrate driven photochemistry of CdSe quantum dot films: Charge injection and irreversible transformations on oxide surfaces, *J. Phys. Chem. A*, **2009**, 113, 3765–3772.

7 A. L. Rogach, Nanocrystalline CdTe and CdTe(S) particles: Wet chemical preparation, size-dependent optical properties and perspectives of optoelectronic applications, *Mater. Scien. and Eng. B*, **2000**, 69-70, 435–440.

8 A. M. Smith, H. Duan, M. N. Rhyner, G. Ruana and S. Nie, A systematic examination of surface coatings on the optical and chemical properties of semiconductor quantum dots, *Phys. Chem. Chem. Phys.*, **2006**, 8, 3895–3903.

9 Y. Li and M. A. El-Sayed, The effect of stabilizers on the catalytic activity and stability of Pd colloidal nanoparticles in the Suzuki reactions in aqueous solution, *J. Phys. Chem. B*, **2001**, 105, 8938–8943.

10 S. Kaniyankandy, S. Rawalekar, S. Verma, D. K. Palit and G. H. N., Charge carrier dynamics in thiol capped CdTe quantum dots, *Phys. Chem. Chem. Phys.*, **2010**, 12, 4210–4216.

11 Y. Kobayashi, L. Pan and N. Tamai, Effect of size and capping reagents on biexciton Auger recombination dynamics of CdTe quantum dots, *J. Phys. Chem. C*, **2009**, 113, 11783–11783.

12 Z. Yuan, A. Zhang, Y. Cao, J. Yang, Y. Zhu and P. Yang, Effect of mercaptocarboxylic acids on luminescent properties of CdTe quantum dots, *J. Fluoresc.*, **2012**, 22, 121–127.

13 H. Zhang, Z. Zhou, B. Yang and M. Gao, The influence of carboxyl groups on the photoluminescence of mercaptocarboxylic acid-stabilized CdTe nanoparticles, *J. Phys. Chem. B*, **2003**, 107, 8–13.

14 D. A. Hines and P. V. Kamat, Quantum dot surface chemistry: Ligand effects and electron transfer reactions, *J. Phys. Chem. C*, **2013**, 117, 14418–14426.

15 A. Iagatti, R. Flamini, M. Nocchetti and L. Latterini, Photoinduced formation of bithiophene radical cation via a hole-transfer process from CdS nanocrystals, *J. Phys. Chem. C*, **2013**, 117, 23996–24002.

16 M. Amelia, R. Flamini and L. Latterini, Recovery of CdS nanocrystal defects through conjugation with proteins, *Langmuir*, **2010**, 26, 10129–10134.

17 Y. Yan, G. Chen, P. G. Van Patten, Ultrafast Exciton Dynamics in CdTe Nanocrystals and Core/Shell CdTe/CdS Nanocrystals, *J. Phys. Chem. C*, **2011**, 115, 22717–22728.

18 M. Sanz, M. A. Correa-Duarte, L. M. Liz-Marzan and A. Douhal, Femtosecond dynamics of CdTe quantum dots in water, *J. Photochem. and Photobiol.*, **2008**, 196, 51–58.

19 S. Kaniyankandy, S. Rawalekar, S. Verma, D.K. Palit, H.N. Ghosh, *Phys. Chem. Chem. Phys.*, **2010**, 12, 4210–4216

20 N. Gaponik, D. V. Talapin, A. L. Rogach, K. Hoppe, E. V. Shevchenko,A. Kornowski, A. Eychmüller and H. Weller, *J. Phys. Chem. B*, **2002**, 106, 7177–7185.

21 S. K. Poznyak, N. P. Osipovich, A. Shavel, D. V. Talapin, M. Gao, A. Eychmüller and N. Gaponik, Thiol-capping of cdte nanocrystals: An alternative to organometallic synthetic routes, *J. Phys. Chem. B*, **2005**, 109, 1094–1100.

22 K. K. Haldar, T. Sen, S. Mandal and A. Patra, Photophysical properties of Au-CdTe hybrid nanostructures of varying sizes and shapes, *ChemPhysChem*, **2012**, 13, 3989–3996.

23 M. Di Donato, A. Iagatti, A. Lapini, P. Foggi, S. Cicchi, L. Lascialfari, S. Fedeli, S. Caprasecca and B. Mennucci, Combined Experimental and Theoretical Study of Efficient and Ultrafast Energy Transfer in a Molecular Dyad, *J. Phys. Chem. C*, 2014, 118, 23476–23486

24 L. Moroni, C. Gellini, P.R. Salvi, A. Marcelli, P.Foggi, Excited States of Porphyrin Macrocycles, *J. Phys. Chem. A*, **2008**, 112, 11044-11051

25 P. L. Gentili, M. Mugnai, L. Bussotti, R. Righini, P. Foggi, S. Cicchi, G. Ghini, S. Viviani and A. Brandi, The ultrafast energy transfer process in naphtole-nitrobenzofurazan bichromophoric molecular systems: A study by femtosecond UV–vis pump-probe spectroscopy, *J. Photochem. Photobiol. A*, **2007**, 187, 209–221.

26 P. L. Gentili, L. Bussotti, R. Ruzziconi, S. Spizzichino and P. Foggi, Study of the Photobehavior of a Newly Synthesized Chiroptical Molecule: (E)-(R_p, R_p)-1,2-Bis{4-methyl-[2] paracyclo[2](5,8) quinolinophan-2-yl} ethene, *J. Phys. Chem. A*, **2009**, 113, 14650–14656.

27 I. M. Bayanov, R. Danielius, P. Heinz and A. Seilmeier, Intense subpicosecond pulses tunable between 4 μm and 20 μm generated by an all-solid-state laser system, *Opt. Commun.*, **1994**, 113, 99–104.

28 R. Danielius, A. Piskarskas, P. Di Trapani, A. Andreoni, C. Solcia and P. Foggi, Visible pulses of 100 fs and 100 μJ from an upconverted parametric generator *Appl. Opt.*, **1996**, 35, 5336–5339.

29 P. Tyagi and P. Kambhampati, False multiple exciton recombination and multiple exciton generation signals in semiconductor quantum dots arise from surface charge trapping, *J. Chem. Phys.*, **2011**, 134, 094706.

30 J. A. McGuire, J. Joo, J. M. Pietryga, R. D. Schaller and V. I. Klimov, New aspects of carrier multiplication in semiconductor nanocrystals, *Acc. Chem. Res.*, **2008**, 41, 1810–1819.

31 H. W. Midgett, H. W. Hillhouse, B. K. Hughes, A. J. Nozik and M. C. Beard, Flowing versus static conditions for measuring multiple exciton generation in PbSe quantum dots, *J. Phys. Chem. C*, **2010**, 114, 17486–17500.

32 C. d. M. Donegá and R. Koole, Size dependence of the spontaneous emission rate and absorption cross section of CdSe and CdTe quantum dots, *J. Phys. Chem. C*, **2009**, 113, 6511–6520.

33 W. W. Yu, L. Qu, W. Guo and X. Peng, Experimental determination of the extinction coefficient of CdTe, CdSe, and CdS nanocrystals, *Chem. Mater.*, **2003**, 15, 2854–2860.

34 Z. J. Jiang and D. F. Kelley, Hot and relaxes electron transfer from the CdSe core and core/shell nanorods, *J. Phys. Chem. C*, **2011**, 115, 4594–4602.

34 M. Laferriére, R. E. Galian, V. Maurel and J. C. Scaiano, Non-linear effects in the quenching of fluorescent quantum dots by nitroxyl free radicals, *Chem. Commun.*, **2006**, 257–259.

36 S. Bhattacharyya, B. Paramanik, S. Kundu and A. Patra, Energy/hole transfer phenomena in hybrid α-sexithiophene (α-sth) nanoparticle-CdTe quantum-dot nanocomposites, *ChemPhysChem*, **2012**, 13, 4155–4162.

37 W. Chen, X. Wang, X. Tu, D. Pei, Y. Zhao and X. Guo, Water-soluble protein-on spin-labeled quantum-dots conjugate, *Small*, **2008**, 4, 759–764.

38 M. Berr, A. Vaneski, C. Mauser, S. Fischbach, A. Susha, A. Rogach, F. Jackel and J. Feldmann, Delayed photoelectron transfer in Pt-decorated CdS nanorods under hydrogen generation conditions, *Small*, **2012**, 8, 291– 297.

39 J.I. Saari, E.A. Dias, D. Reifsnyder, M.M. Krause, B.R. Walsh, C.B. Murray, P. Kambhampati, Ultrafast Electron Trapping at the Surface of Semiconductor Nanocrystals: Excitonic and Biexcitonic Processes, *J. Phys. Chem B*, **2013**, 117, 4412-4421

40 V. I. Klimov, D. W. McBranch, C. Leatherdale and M. G. Bawendi, Electron and hole relaxation pathways in semiconductor quantum dots, *Phys. Rev. B*, **1999**, 60, 13740–13749.

41 V. I. Klimov, A. A. Mikhailovsky, S. Xu, A. Malko, J. A. Hollingsworth, C. A. Leatherdale, H.-J. Eisler and M. G. Bawendi, Optical gain and stimulated emission in nanocrystal quantum dots, *Science*, **2000**, 390, 314–317.

42 V. I. Klimov, Optical nonlinearities and ultrafast carrier dynamics in semiconductor nanocrystals, *J. Phys. Chem. B*, **2000**, 104, 6112–6123.

43 M. T. Trinh, A. J. Houtepen, J. M. Schins, T. Hanrath, J. Piris, W. Knulst, A. P. L. M. Goossens and L. D. A. Siebbeles, In spite of recent doubts carrier multiplication does occur in PbSe nanocrystals, *Nano Lett.*, **2008**, 8, 1713–1718.

44 L. Padilha, A. Neves, C. Cesar and L. Barbosa, Recombination processes in CdTe quantum-dot-doped glasses, *Appl. Phys. Lett.*, **2004**, 85, 3256–3258.

Table 1. Molar extinction coefficient of CdTe QDs in water at different wavelengths.

MPA-CdTe		**TG-CdTe**	
ε_{400} = 748000	[QDs] = 3.4×10^{-6}	ε_{400} = 545000	[QDs] = 5.3×10^{-6}
ε_{565} = 198000	[QDs] = 3.6×10^{-6}	ε_{520} = 215000	[QDs] = 5.5×10^{-6}

Table 2. Band gap position, FWHM of the luminescence band, Stokes shift and luminescence QY of CdTe as a function of the capping agent.

Sample	**BG (nm) [eV]**	**FWHM (cm^{-1})**	**Stokes shift (cm^{-1})**	**QY (%)**
MPA-CdTe	565 [2.19]	1840	890	17
TG-CdTe	518 [2.39]	1820	1420	10

Table 3. Luminescence decay parameters for CdTe QDs in water obtained from TCSPC measurements.

Sample	**τ_{1L} (ns)**	**A_1 (%)**	**τ_{2L} (ns)**	**A_1 (%)**	**$< \tau_L >$ (ns)**	**χ_{sq}**
MPA-CdTe	7.1	49.0	30.1	51.0	25.8	0.98
TG-CdTe	20.8	58.9	51.6	41.1	40.3	1.03

Table 4. Fitting parameters (decay time and relative weight) of transient absorption decay traces at selected probe wavelengths recorded for CdTe QDs in water using different pump wavelengths.

MPA-CdTe										
λ_{pump} (nm)	λ_{probe} (nm)	A_1 (%)	τ_1(ps) ±S.D.	A_2 (%)	τ_2(ps) ±S.D.	A_3 (%)	τ_3(ps) ±S.D.	A_4 (%)	τ_4 (ns)	$\tau_{ESA}^{660}(ps)$ ± S. D.
400	460	0	0	87	1.6±0.2	3	30 ±3	10	25.8	1.4±0.1
	520	-44	0.41±0.05	26	1.8±0.1	12	16±1.8	18		
	565	-47	0.61±0.02	34	0.9±0.07	8	20±1	10		
	600	-72	0.80±0.09	6	1.0±0.1	9	25±2	13		
520	565	-14	0.32±0.06	33	6.7 ±0.8	12	129±10	41	25.8	1.5 ±0.3
	600	-31	0.33±0.07	28	12 ±1.3	11	140±14	30		
TG-CdTe										
λ_{pump} (nm)	λ_{probe} (nm)	A_1 (%)	τ_1(ps) ±S.D.	A_2 (%)	τ_2(ps) ±S.D.	A_3 (%)	τ_3(ps) ±S.D.	A_4 (%)	τ_4 (ns)	$\tau_{ESA}^{660}(ps)$ ± S. D.
374	480	-50	0.58±0.09	49	0.6±0.1	0.5	9.0±1.5	0.8	40.3	3.2±0.7
	520	-50	0.47±0.06	26	1.1±0.13	10	12±1.3	15		
	540	-51	0.70±0.08	35	1.1±0.12	7	16±1.8	8		
476	520	-6	0.33±0.07	28	2.0±0.3	21	14±2.5	45	40.3	low signal
	540	-12	0.36±0.06	32	2.7±0.3	18	15±2	38		
	560	-21	0.40±0.09	41	5.8±0.7	6	16±4	32		

Figure Captions

Figure 1: Absorption (black line) and luminescence spectra (red line) of MPA-CdTe (A, λ_{exc} = 565 nm) and TG-CdTe (B, λ_{exc} =520 nm) QDs in water; inset TEM images of the samples (scale bar correscopnds to 30 nm)

Figure 2: (A) Transient absorption spectrum (red line) of MPA-CdTe recorded 3 ps after the excitation pulse (λ_{pump} =520 nm) compared to the stationary absorption spectrum (blue line); (B) signal decay traces at selected probe wavelengths.

Figure 3: (A) Transient absorption spectrum (red line) of MPA-CdTe recorded 3 ps after the excitation pulse (λ_{pump} = 400 nm) compared to the stationary absorption spectrum (blue line); (B) signal decay traces at selected probe wavelengths.

Figure 4: (A) Transient absorption spectrum (red line) of TG-CdTe recorded 3 ps after the excitation pulse (λ_{pump} = 476 nm) compared to the stationary absorption spectrum (blue line); (B) signal decay traces at selected probe wavelengths.

Figure 5: (A) Transient absorption spectrum (red line) of TG-CdTe recorded 3 ps after the excitation pulse (λ_{pump} = 374 nm) compared to the stationary absorption spectrum (blue line); (B) signal decay traces at selected probe wavelengths.

Figure 6: Transient spectra of (A) MPA-CdTe (λ_{pump} = 400 nm) and (B) TG-CdTe (λ_{pump} = 374 nm) nanocrystals at different delays

Figure 7: Scheme of the electronic transition and recombination processes occurring in TG- and MPA-CdTe QDs

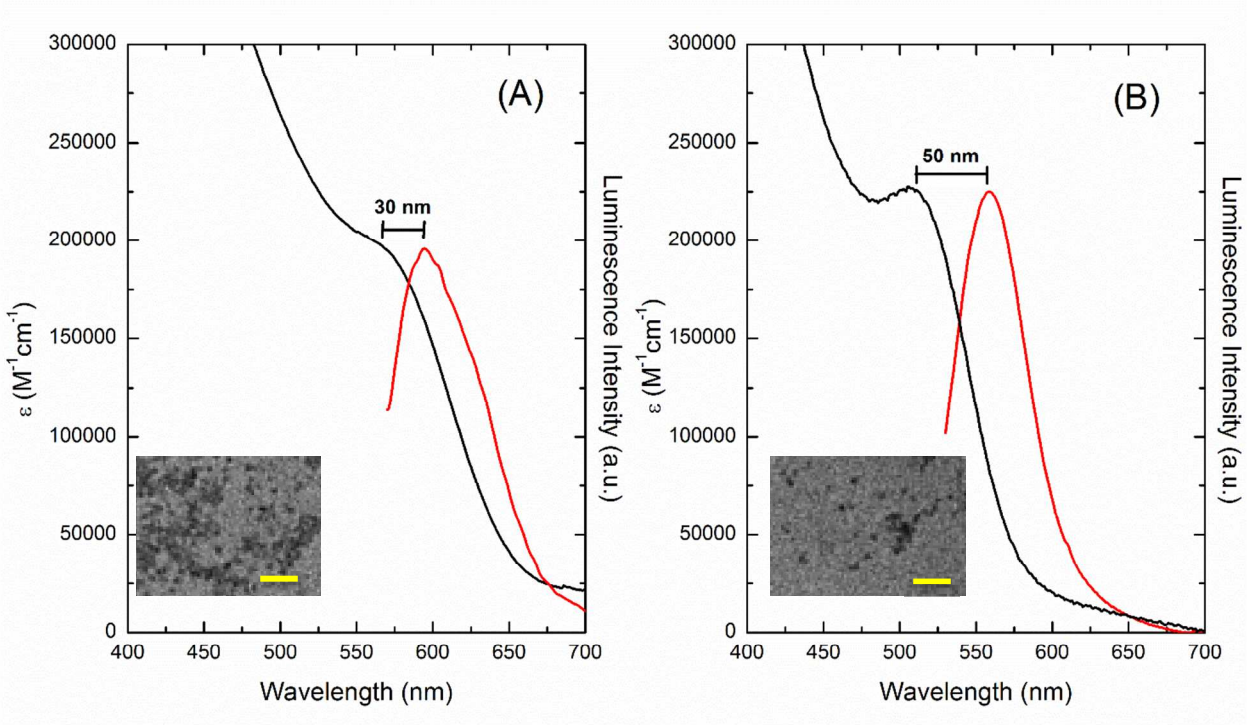

Figure 1: Absorption (black line) and luminescence spectra (red line) of MPA-CdTe (A, λ_{exc} = 565 nm) and TG-CdTe (B, λ_{exc} =520 nm) QDs in water; inset TEM images of the samples (scale bar correscopnds to 30 nm)

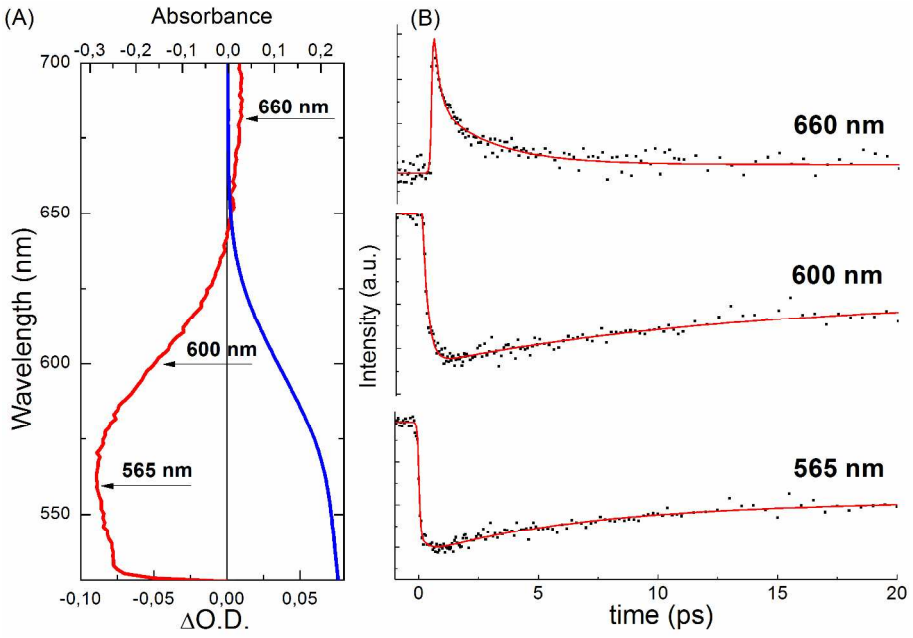

Figure 2: (A) Transient absorption spectrum (red line) of MPA-CdTe recorded 3 ps after the excitation pulse (λ_{pump} =520 nm) compared to the stationary absorption spectrum (blue line); (B) signal decay traces at selected probe wavelengths.

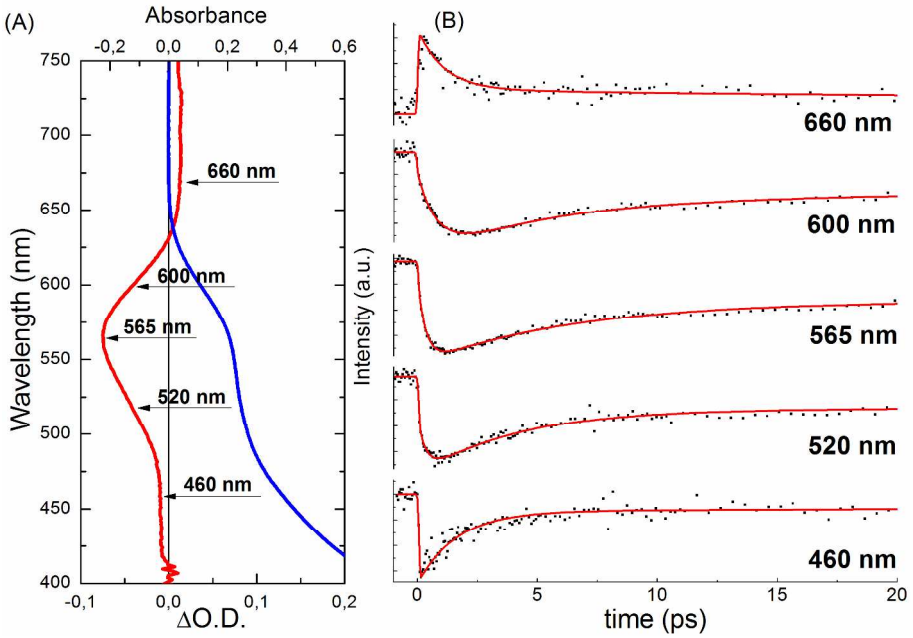

Figure 3: (A) Transient absorption spectrum (red line) of MPA-CdTe recorded 3 ps after the excitation pulse (λ_{pump} = 400 nm) compared to the stationary absorption spectrum (blue line); (B) signal decay traces at selected probe wavelengths.

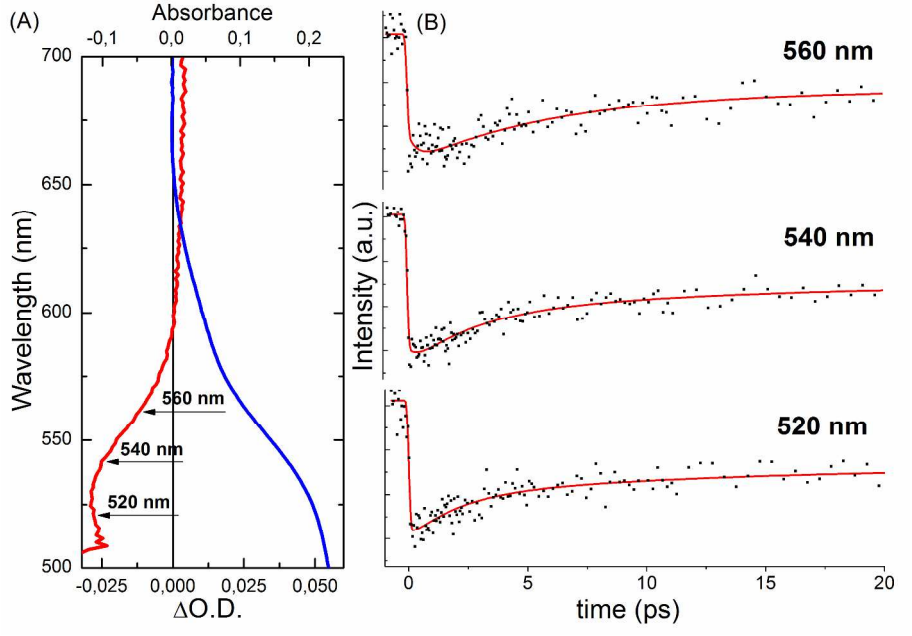

Figure 4: (A) Transient absorption spectrum (red line) of TG-CdTe recorded 3 ps after the excitation pulse (λ_{pump} = 476 nm) compared to the stationary absorption spectrum (blue line); (B) signal decay traces at selected probe wavelengths.

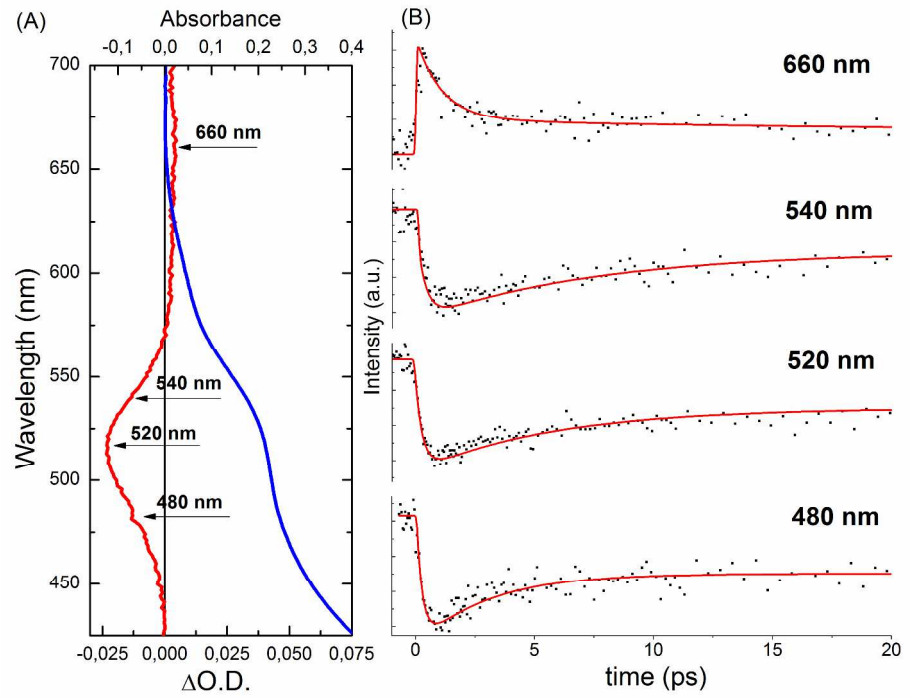

Figure 5: (A) Transient absorption spectrum (red line) of TG-CdTe recorded 3 ps after the excitation pulse (λ_{pump} = 374 nm) compared to the stationary absorption spectrum (blue line); (B) signal decay traces at selected probe wavelengths.

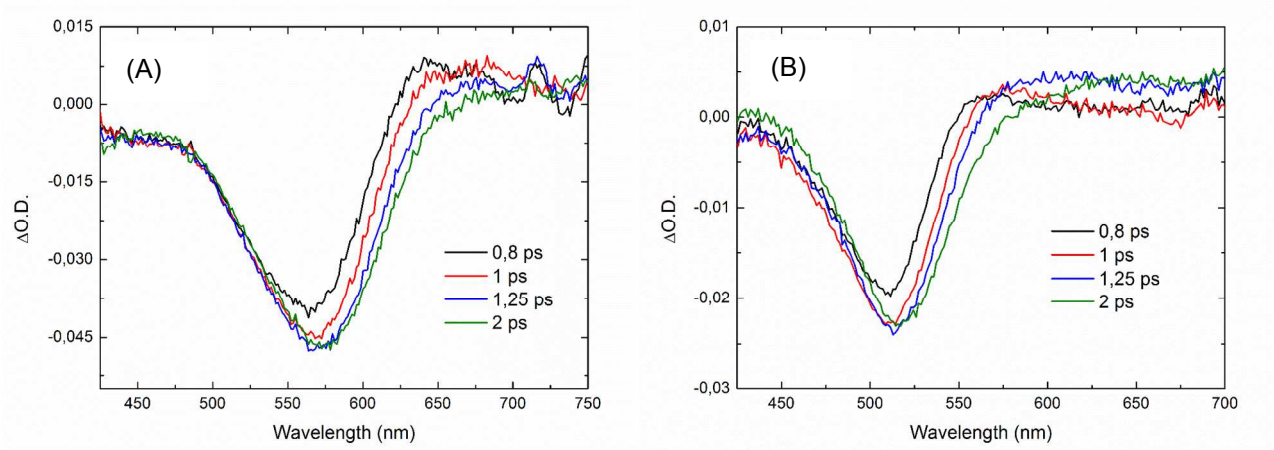

Figure 6: Transient spectra of (A) MPA-CdTe (λ_{pump} = 400 nm) and (B) TG-CdTe (λ_{pump} = 374 nm) nanocrystals at different delays

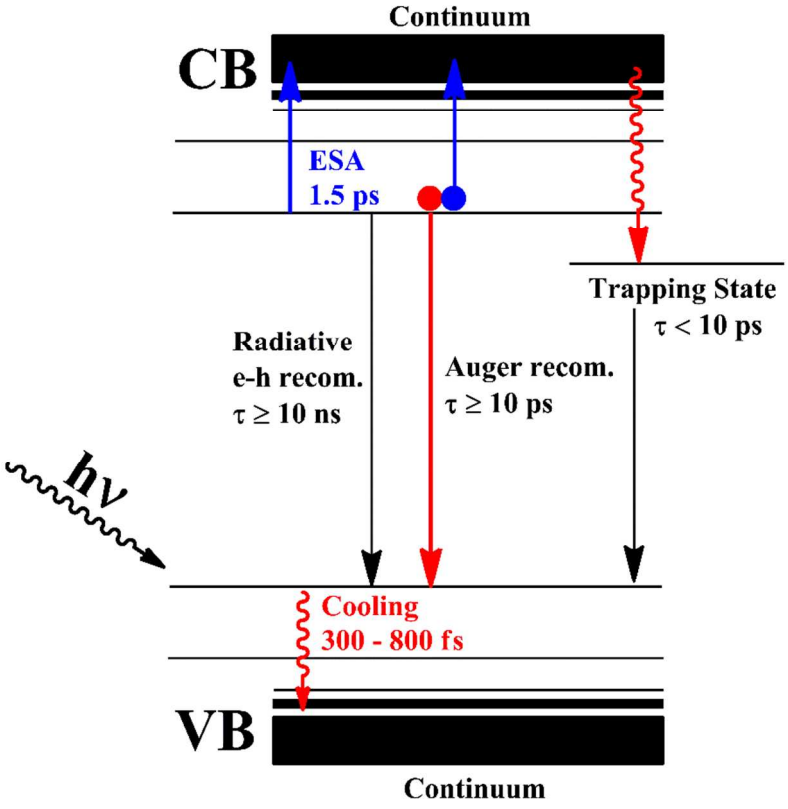

Figure 7: Scheme of the electronic transition and recombination processes occurring in TG- and MPA-CdTe QDs

Steady state and time-resolved photophysical study of CdTe quantum dots in water.

Alessandro Iagatti,[a;b] Luigi Tarpani,[c] Eleonora Fiacchi,[c] Laura Bussotti,[a] Agnese Marcelli,[a] Paolo Foggi[a;b;c] and Loredana Latterini[c*]*

[a]European Laboratory for Non Linear Spectroscopy (LENS), Università di Firenze, via Nello Carrara 1, 50019 Sesto Fiorentino, Florence, Italy

[b]INO-CNR, Istituto Nazionale di Ottica – Consiglio Nazionale delle Ricerche, Largo Fermi 6, 50125 Florence, Italy

[c]Dipartimento di Chimica, Biologia e Biotecnologie and Centro Eccellenza Materiali Innovativi Nanostrutturati (CEMIN), Università di Perugia, Via Elce di Sotto 8, 06123 Perugia, Italy

E-mail: loredana.latterini@unipg.it ; foggi@lens.unifi.it